CONF-771035--7

PREPRINT UCRL- 98[illegible]

Lawrence Livermore Laboratory

[illegible]

[illegible]

[illegible]

[illegible]

This is a preprint of a paper intended for publication in a journal or proceedings. Since changes may be made before publication, this preprint is made available with the understanding that it will not be cited or reproduced without the permission of the author.

MASTER

[illegible]

[illegible]

[illegible]

[illegible]

Abstract

Conditions for the stable propagation of a [illegible] [illegible] [illegible] torr) [illegible] [illegible]

Introduction

[illegible]

assumed to scale as $\nu_m = \nu_{mo}\, p$. The peak growth rate, occurring at $k_\parallel = \omega_{pe}/v_B$, is given approximately as the lower of the collisional (C) or collisionless (MC) forms:

$$\mathrm{Im}(\omega)_C = \frac{\omega_{pi}}{\gamma^{3/2}}\left[\frac{\omega_{pe}^2(\gamma^2\sin^2\theta + \cos^2\theta)}{2\nu_m}\right]^{1/2}, \tag{2a}$$

$$\mathrm{Im}(\omega)_{MC} = \frac{\sqrt{3}}{2}\left[\frac{\omega_B^2\,\omega_{pi}^2(\gamma^2\sin^2\theta + \cos^2\theta)}{\gamma^3}\right]^{1/3}. \tag{2b}$$

The two-stream mode is stabilized when the phase-mix damping due to spread beam velocity becomes comparable to the collisional, cold-beam growth rate;[3] the approximate criterion being $\mathrm{Im}\omega_{MC} \le \mathrm{Im}\omega_C$. When for the cold beam the collisional growth rate is appropriate, the condition $\mathrm{Im}(\omega)_{MC} \le \underline{\omega}\cdot\underline{w}$ defines the transition to the kinetic regime for the instability and growth rates are reduced. However, the condition for stabilization requires $\mathrm{Im}(\omega)_C \le \underline{\omega}\cdot\underline{w}$. Transverse spread ($\Delta v_\perp$) is due to particle oscillations in the pinch field, which we take as $\Delta v_\perp/v_B = (I_b/2I_A)^{1/2}$, with I_A = 17000 Amps. For a nonadiabatic beam $\Delta v_\perp/c = \Delta r_b^2/(2e^2)$. Because the beam has finite radius (R), we set $k_\perp = R^{-1}$, this lowest $k_\perp$ mode being the most difficult to suppress. For maximum growth, $k_\parallel = \omega_{pe}/v_B$.

Equating $\mathrm{Im}(\omega)_C$ with $\underline{\omega}\cdot\underline{w}$ gives the stability boundary:

$$\frac{\omega_{pi}}{\gamma^{3/2}}\left[\frac{\omega_{pe}^2(\gamma^2/R^2 + \omega_{pe}^2/v_B^2)}{2\nu_{mo}(1/R^2 + \omega_{pe}^2/v_B^2)}\right]^{1/2} = c\left[\frac{1}{R}\left(\frac{\omega_{pi}}{2\omega_{pe}}\right)^{1/2} + \frac{\omega_{pi}}{\nu_{mo}}\frac{\omega_{pe}}{\omega_{pi}}\right]. \tag{3}$$

Taking fixed beam parameters (I_b, γ, R), we locate the stability boundary of pressure as P depends on n_e. This curve is denoted $\hat{P}(n_e)$. For fixed pressure there is stability for sufficiently high plasma density because $\mathrm{Im}(\omega)_C \propto n_e^{1/4}$, while the phase mixing term $\underline{\omega}\cdot\underline{w} \propto \omega_{pe} = n_e^{1/2}$. At low plasma density the mode is also stabilized, because the

loses little current in this process. We have verified this effect analytically and with the relativistic particle simulation code ZOO.[4] Current gains $(I_{max}/I_b) \sim 1.5$ for the weakly relativistic diode beam and ~ 2.5 for the highly relativistic Astron beam are indicated.

It is apparent that the critical pressure for stability should depend on gas type primarily through the value of ν_{no}, i.e. $p_c \propto \nu_{no}^{-1}$. Experimentally it is observed that $p_c \propto \nu_{io}^{-1}$, where ν_{io} is the ionization rate for 100 eV electrons in the gas type considered at 1 torr. We explain this observation by the fact that electron temperatures are in excess of 10 eV, where $\nu_{io} \propto \nu_{no}$. That is, the scaling with ν_{io} is in accord with our predicted scaling with ν_{no}.

Numerical Model of Resistive Regime

ZOOMSE treats a highly relativistic beam propagating in gas characterized by scalar conductivity σ. There is no consideration of microinstability. Current is small compared with the Alfvén limit, so the paraxial approximation for beam dynamics is adopted. The code is described in greater detail in Ref. (5); the principal features are as follows:

(1) The fields are derived from two components of potential (A_z and ϕ), with Maxwell's equations solved assuming the field pattern propagates at the speed of light.[6]

(2) Conductivity is $\sigma = n_e e^2/m\nu_m$, with $\nu_m = 6.4 \times 10^9/(\text{torr-s})$. Electron density is generated according to

$$\frac{\partial n_e}{\partial t} = k\, n_g \frac{|J_b|}{e} + \nu_i n_e ,$$

with effective ionization cross section $k = 1.3 \times 10^{-18}$ m^2, and avalanche rate ν_i is a function of $|E/p|$ fitted to air breakdown data.[7] Recombination is neglected.

(5) The beam is composed of 300-500 segments of varying thickness Δx which are advanced at the speed of light in z and do not intermix. Each segment is itself composed of 100 disks of distributed mass in order to simulate the phase mixing effects of particle orbits in the anharmonic pinch field.[6] The transverse acceleration of the i^{th} disk is

$$\frac{d^2y_i}{dz^2} = \frac{e}{\gamma_i m}\overline{E_\perp(R_b - e)} \qquad (i = 1, \ldots, 100) , \qquad (11)$$

with the mean taken over the displaced disk profile. The mean displacement for the whole segment $\bar{y}$ is a weighted mean of the y_i.

Computational Results

EXPULSE runs were made to simulate the diode experiments at pressures of 2, 5, 10, 20 and 200 torr air. All runs are made with parameters $b = 4.95$ cm, $I_0 = 10$ kA, $L_p = 120$ cm, $\lambda_p = 1200$ cm, and $\gamma = \infty$. Emittance was selected such that the fully pinched radius was $R = 1$ cm. At the point of injection ($z = 0$) a perturbation of the form $y_i(x) = \cos(\pi x/\lambda_p)$ was applied. The entire pulse was then propagated to $z_{max} = 400$ cm.

Table 1 gives the most significant computed equilibrium quantities (z independent) for the representative point $x = 600$ cm. The "pinch point" is the position in the beam head at which self-focusing effects first create the pinch equilibrium. This is somewhat of an artifice in the manner in which the profile is handled, but it is considered a reasonable indicator of the "true beginning" of equilibrium. "Maximum displacement" gives the largest displacement $\bar{y}(z, x) = Y_{max}$, computed near the pulse midpoint at $x = 600$ cm. Since the perturbation equations are linear, Y_{max} should be compared with the initial perturbation amplitude of unity. The "amplification point" gives the x-point in the pulse where

(1) In all runs, ionization is due primarily to the direct process for the first 10 cm of pulse. Hence, the ionization point is similar for all.

(2) In all runs, net current is close to beam current through the first 10 cm of pulse; thereafter, in the low pressure runs, the inductance of coils to "freeze in" net current, causing I to fall well below I_b in the body of the pulse. But for high pressure, $I = I_b$ throughout the pulse.

(3) Beam radius should be given approximately by IR^2 = constant. This is qualitatively borne out.

(4) The product $n_e\mu^2$ is nearly independent of p for the low pressure runs; the breakdown process appears to remove a constant amount of energy from the pulse. Hence, σ and λ vary as p^{-1}, since $\nu_m \propto p$.

(5) In the pulse body, the maximum ionization front point x_m to x is predicted by a simple analytic model[9] to be

$$Y_{max}(x) = \left(\frac{x}{x_0}\right)^{\frac{\sigma_0}{\partial\lambda/\partial x}} . \qquad (13)$$

Values of Y_{max} derived from this formula, using the mean value of $\partial\lambda/\partial x$, are given in Table 3. We take x_0 to be the point at which growth is first observed, and we take x = 600 cm, the point where Y_{max} is computed. An approximate agreement between BOOSTER runs and this formula is evident.

(6) In all runs except p = 200 torr the pulse head is stable. This is a new feature in the face instability picture provided by BOOSTER but not yet fully understood. It is known that face growth should be stabilized at very low conductivity ($\omega\tau/c < 1$), which prevails at the ionization point. For the remainder of the pulse head it is [illegible] that the rapid decrease of the effective betatron period with [illegible] point causes a "net gain" of the instability, with [illegible] sion of growth.

5. R. Briggs, J. Clark, T. Fessenden, E. Lee and E. Lauer, Stable Propagation of A High-Current Electron Beam: Experimental Observations and Computational Modeling, Lawrence Livermore Laboratory, Livermore, Ca., UCID-17516, 1977.

6. E. P. Lee, The New Field Equations, Lawrence Livermore Laboratory, Livermore, Ca, UCID-17266, 1976.

7. P. Felsenthal and J. M. Proud, Physical Review, 139 (6A) 1796(1965).

8 E. P. Lee, Resistive Hose Instability of a Beam with the Bennett Profile, submitted to Physics of Fluids for publication.

9. R. J. Briggs, E. P. Lee, and L. D. Pearlstein, Resistive Hose Instability of a Pulsed Relativistic Electron Beam, in preparation for publication in Physics of Fluids.

Table 1. Computed behavior of beam-plasma system at several pressures. Net current, conductivity, electron density and beam radius are given for the point x = 500 cm. Conductivity and density are on-axis values. Maximum displacement is given for x = 600 cm point.

Gas pressure, Torr	Net current,* A	Electrical conductivity,* sec^{-1}	Electron density,* cm^{-3}	Beam radius,* cm	Pinch point, cm	Maximum displacement x = 600 cm	Amplification point cm
2	3980	4.9×10^{12}	2.5×10^{14}	2.01	9.4	1.0	—
5	4980	3.2×10^{12}	4.1×10^{14}	1.66	8.6	1.7	400
10	6250	2.3×10^{12}	5.9×10^{14}	1.38	8.9	3.5	225
20	7790	3.0×10^{12}	8.0×10^{14}	1.17	9.7	4.5	175
200	9600	5.6×10^{11}	5.0×10^{15}	1.02	12.4	200+	55

*Given for the point x = 500 cm.

Table 2. Dipole decay length vs pressure. Here $\lambda = \pi a^2/2c$ and $d\lambda/dx \approx \lambda/500$ cm is a rough mean through the pulse.

Pressure, Torr	2	5	10	20	200
λ, cm	1036	461	233	215	53.4
$d\lambda/dx$	2.07	0.923	0.465	0.430	0.106

Table 3. Comparison of the analytic estimate of hose growth with the growth computed with EMPULSE.

Pressure, Torr	2	5	10	20	200
Analytic estimate	–	1.4	4.3	7.2	6×10^5
EMPULSE	–	1.7	3.5	4.5	200+

growth rate again varies as $n_e^{[illegible]}$ but the mixing term approaches a constant.

Results are presented for [illegible] parameters in Figs. (1, 2). Specifically we set I_b = 10 kA, γ = 3.0, P = 1 cm. ν_{en} is taken to be 6.4×10^7/(torr-s), which is valid for 2-10 eV electrons in air. Figure (1) gives $p(n_e)$ and also indicated are the zones where the mode is respectively collisional, collisionless, or kinetic. Sufficiently high pressure ($p \geq$ [illegible] torr) results in complete suppression of the mode. At intermediate pressures the mode is unstable for a finite range of n_e but stabilized in excess of this range are produced [illegible] by the beam. Note that, as the pressure is lowered below ~ 1 torr, the density required for suppression rises very rapidly. It is this very rapid rise in required plasma density, coupled with the reduced density production by classical mechanisms at lower pressures which leads to the critical pressure $p_c \approx 2$ torr.

In Fig. (2), the measured plasma density and that computed with [illegible] are plotted along with the stability boundary from Fig. (1). Above 2 torr the plasma production by direct ionization and avalanche ionization are sufficient to suppress the mode during most of the pulse. Below 2 torr quite high densities are required and such large densities are in fact observed. However, the numerical agreement in the range 1-2 torr is actually fortuitous. The two stream mode does not directly break down the gas to such high densities; rather, it produces a hot electron component in the plasma. These hot electrons then [illegible] the gas on a longer time scale (~1 μs) than the ~50 ns beam pulse length.

The two-stream interaction can lead to a marked increase in the net current because momentum is transferred from the beam to the plasma electrons, thus building up plasma current. The beam, being relativistic, [illegible]

(3) For the unperturbed current profile a truncated Bennett form is adopted (in accord with recent measurements[?]):

$$J_{z0}(r, x) = \frac{I_b(x)}{\pi R^2} \left(1 + \frac{r^2}{R^2}\right)^{-2} \left(1 - \frac{r^2}{b^2}\right)^2 NORM, \qquad (5)$$

where R(x) is scale radius, b is channel radius and NORM is a normalization factor. These quantities depend on z and t only through the Doppler shifted time variable $x = ct - z$. Beam current is

$$I_b(x) = I_0 \tanh\left(\frac{x}{x_r}\right) \tanh\left(\frac{x_p - x}{x_r}\right) , \qquad (6)$$

where x_r is rise length and x_p is pulse length. Radius R(x) is determined from the balance between finite emittance (ε) and the pinch force:

$$\epsilon^2 = R^2 \frac{e}{\gamma m c^2} \overline{(rE_r - rB_\theta)} . \qquad (7)$$

with the average taken over the beam profile. Since E_r and B_θ tend to cancel at the nose ($x = 0$), this is a zone where no equilibrium is found. We somewhat arbitrarily set $R = 10$ cm if the emittance condition Eq. (7) cannot be satisfied by a smaller radius.

(4) To treat hose instability the functions A_z, φ and ρ are decomposed into azimuthal components:

$$A_z(r, \theta, x, z) = A_{z0}(r, x) + A_{z1}(r, x, z)\cos\theta , \qquad (8)$$

etc., and the beam current has the form resulting from a rigid displacement $\bar{y}$:

$$J_b(r, \theta, x, z) = J_{b0}(r, x) - \bar{y}(x, z) \frac{\partial J_{b0}}{\partial r} \cos\theta , \qquad (9)$$

the oscillations begin to exceed the initial perturbation. Before this point, $\bar{y}$ shows only damped oscillatory behavior.

In Table I, the appropriate radiolic decay length (λ) at the point $x = 500$ cm is given. Its mean derivative w.r.t. x is also estimated:

$$\lambda = \frac{\pi a^2}{2c} \cdot \frac{d\lambda}{dx} \approx \frac{\lambda}{x} . \qquad (11)$$

These quantities are useful in the interpretation of computed burn growth. For comparison we note that, with direct ionization alone ($\nu_i = 0$), the conductivity rise is such that

$$\left(\frac{d\lambda}{dx}\right)_{direct} \approx 0.1 . \qquad (12)$$

Discussion of Results and Comparisons with the Experiments

The input for the five runs differ only in gas pressure. Hence, if ν_i vanished, all the runs would be identical. The considerable differences among the runs can, therefore, be ascribed to the avalanching process, which is dominant at $p = 2$ torr and negligible at 760 torr.

The degree of ionization calculated by EXPLORE is in good agreement with the experimental measurements. In Fig. 2 the computed density (from Table I) is plotted along with experimental observations. At 200 torr, recombination begins to limit plasma density, but this is not included here.

The general pattern of the predictions for beam amplification is also in agreement with the experimentally determined beam pulse energy on a calorimeter (at 300 cm). In Fig. (3) this plot is overlaid with the computed amplification factor (W_{max}/W_0), 400 cm into plasma. The high-pressure side of the stable window is thus accounted for by increased beam disruption with increasing pressure.

Some additional comments on the code results follow:

(7) Mode growth is delayed by rapid growth of σ; note that the position at which mode amplification begins (x_0) increases as p is reduced. This fact is explained by the competition between phase-mix damping and unstable growth. The damping always prevails at small x, so as mode growth is reduced, the damped zone is expanded.

(8) Finally, it is important to note that the run at p = 2 torr shows no mode growth at all. [illegible] can be run at even lower pressures, but the results cannot be in accord with experiment. A preliminary study shows that the trend of increasing λ with decreasing p continues at least to 0.1 torr. No "saturation" of the secondary ionization is observed in the computer runs, so [illegible] propagation [illegible] in the [illegible] experiments does not appear to be related to mode instability.

Acknowledgements

Work supported by USERDA, contract no. [illegible] and Dept. of Navy, contract no. [illegible].

References

1. T. J. Fessenden, et al., Companion paper presented at this conference.

2. S. A. Bludman, K. M. Watson, M. N. Rosenbluth, Phys. Fluids Vol. 3, No. 5 September-October 1960, p 747.

3. R. J. Briggs, in Advances in Plasma Physics, Vol. 4, A. Simon and W. B. Thompson, ed., Interscience Publishers, New York (1971) p 43.

4. E. J. [illegible], Phys. Fluids, [illegible]

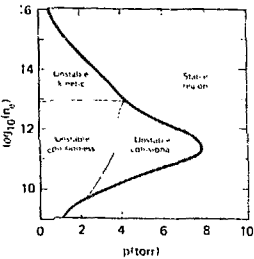

Fig. 1 Regions of instability vs n_e and p for I_B = 10,000 A, R = 1 cm, γ = 3.0.

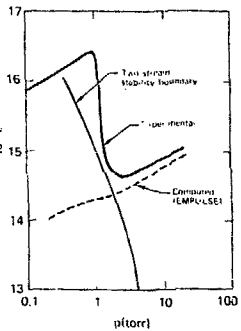

Fig. 2 Comparison of experimental and classically computed density vs pressure with the boundary for stability of the two stream interaction.

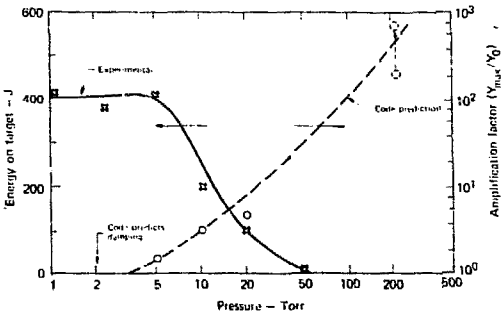

Fig. 3 Experimentally determined beam pulse energy on target at 100 cm and EMPULSE code prediction of amplification factor vs pressure.